



## **Synthesis, Growth, Spectral, Optical, Thermal, and Non-Linear Optical Applications of an Inorganic Single Crystal: Potassium Dihydrogen Orthophosphate- Sodium Chloride Single Crystal**

**S. Jeeva, K. Arulaabaranam, S. Chithra, K. Selvam, G. Mani\***

**PG & Research Department of Physics, Arignar Anna Government Arts College -  
Cheyyar- 604 407, Tamil Nadu, India.**

**Abstract :** An inorganic nonlinear optical substantial of a single crystal of Potassium dihydrogen phosphate - Sodium chloride [PDPSC] is synthesized by slow evaporation method at room temperature. The blended material is exposed to single-crystal X-ray diffraction analysis to classify the atomic unit cell fundamental parameters. As grown crystal to ascertain the fundamental functional groups find by Fourier transform infrared spectrum. The fingerprint Raman spectra of the grown crystal is quality and impurity has been discussed. Optical absorption studies illustrate low absorption in the entire UV and visible region with a lower cut off wavelength of 240 nm and there by optical band gap energy  $E_g$  is calculated to be 5.126 eV. The Surface morphology of the crystallized salt also examines studies with different magnification. Grown crystal elemental compositions were identified by energy dispersive X-ray spectroscopy. Fingerprint techniques of Raman spectroscopy also added to examine the crystalline quality and the functional group of the materials. The Kurtz powder SHG was confirmed using Nd:YAG laser with fundamental wavelength of 1064 nm. The relative second harmonic efficiency of the compound found to be 1.61 times less than that of KDP. Thermal stability of the grown crystal vividly studied by thermo gravimetric analysis and differential scanning calorimetric techniques measurements. The Photoluminescence spectrum exhibited three peaks (427 nm, 620 nm, 759 nm) study at certain energy can be viewed as transition energy from the grown crystal.

**Keywords :** Optical, Structural, Thermal Properties, Morphological Studies, NLO.

### **1. Introduction**

Potassium di hydrogen phosphate (KDP) is a technologically important inorganic NLO crystal. It has been received special attention of research community because of its uniqueness in unique nonlinear optical and ferroelectric properties [1]. Growth of nonlinear optical (NLO) Single crystal with good quality initiates the development of many novel devices in the field of optoelectronics and optical communication such as optical modulator, optical data storage and optical switches [2, 3]. NLO materials have large non linearity, high resistance, too large induced damage, low angular sensitivity and good mechanical hardness [4]. Organic crystals can exhibit higher nonlinear optical efficiencies than those inorganic materials due to large optical susceptibilities, high optical threshold for laser power and low frequency dispersion [5,6]. Potassium dihydrogen phosphate (KDP) and its isomorphs are representatives of hydrogen bonded materials that possess important piezoelectric, ferroelectric, electro-optic and nonlinear properties. They have attracted interest of

many theoretical and experimental researchers probably because of their comparatively simple structure and very fascinating properties associated with a hydrogen bond system involving a large isotopic effect, broad transparency range, a high laser damage threshold and relatively low production cost [7,8]. The rapid growth of good quality crystals and various studies of organic and inorganic impurities doped KDP crystals have been reported by various studies and various investigated [9-19]. In this present work an attempt has been made to grow long size transparent PDPSC crystal by slow evaporation solution growth technique. The grown crystals were characterized by SXRD, FTIR, FT-Raman, UV-visible, SEM, EDAX, NLO Properties, TG/DSC and PL measurements.

## 2. Materials and methods

### 2.1. Synthesis and crystal growth of PDPSC

Potassium dihydrogen orthophosphate and sodium chloride was synthesized by taking commercially available (AR grade E-Merck) Potassium dihydrogen orthophosphate and sodium chloride in the ratio of 1:1 mole dissolved in double distilled water at room temperature. The saturated solution with continuous stirring 6hrs. The PH of the PDPSC solution has been identified in PH value 7. Then after the saturation solution was filtered using filter paper and kept in a petri dish allowed to grow seed crystal within 10-15 days. The grown crystal seems colorless and transparent closely with standard once. **Fig.1.** Shows typically view of single crystalline of PDPSC crystal grown by slow evaporation technique.



**Fig. 1.** As grown of bulk PDPSC single crystal

### 2. 2. Characterization techniques

The grown transparent crystal harvested good quality with single crystal line of PDPSC were subjected to various analytical characterization methods like single crystal X-ray diffraction, Fourier transform infrared (FTIR), FT-Raman, UV-visible, SEM, EDAX, PL, TG/DSC and NLO studies. The lattice unit cell parameters of the grown PDPSC crystal has been found for a BRUKER KAPPA APEX II CCD diffractometer employing  $M_0K_\alpha$  ( $\lambda=0.71073\text{\AA}$ ) radiation. FTIR spectrum was recorded using PERKIN ELMER spectrometer in the range  $4000-400\text{cm}^{-1}$  by KBr pellet technique. Powder FT-Raman spectrum was recorded on a BRUKER RFS 27 spectrometer in the range  $4000-450\text{cm}^{-1}$ . The optical absorption spectrum for the grown crystal is recorded in the range  $200\text{nm}-700\text{ nm}$  using variation Cary 5E UV-Visible NIR Spectrometer. The surface morphology natures of the grown crystal analysis have been studied by scanning electron microscope (SEM) measured by Carl Zeiss, The TG/ DSC of PDPSC has been recorded by using NETZSCH STA 449F3 thermal analyzer at a heating rate of  $20^\circ\text{C min}^{-1}$  in the temperature range of  $20^\circ$  to  $1200^\circ\text{C}$ . Photoluminescence spectrum of PDPSC also recorded using PERKIN ELMER LS-45 Spectrofluorophotometer in the range  $300-700\text{ nm}$ . Also analysis the nonlinear optical property of PDPSC, powder sample is exposed to pulsed Nd :YAG laser using Kurtz Perry powder method.

### 3. Result and discussion

#### 3.1. Single crystal X-ray diffraction

The single crystal X-ray diffraction (XRD) used for the grown PDPSC crystal has been carried out to confirm the crystallinity and identify the unit cell parameters. It exhibits with space group is Tetragonal I crystal system. The lattice parameters are calculated from single crystal data and the calculated values are given in **Table. 1**. Along with values in reported in literature [20] for the sake of comparison. The calculated values are in good agreement with reported work.

**Table. 1. Single crystal XRD data of PDPSC**

Cell parameters	Present work	Reported work [20]
Space group	Tetragonal I	Tetragonal I
a (Å)	7.50	7.45
b (Å)	7.50	7.45
c (Å)	7.03	6.97
volume(A <sup>3</sup> )	396387.62	
$\alpha=\beta=\gamma$ ( °)	90	90

**Table. 2. Functional group assignments for PDPSC single crystal are listed in the table.**

Frequency wavenumber (cm <sup>-1</sup> )		Band assignments
FT-IR	FT-Raman	
3660	3632	O-H Free stretching
2941	2926	P-O-OH asymmetric stretching
2436	2428	O=P-OH asymmetric stretching
1300	1260	P=O stretching
1097	1094	P=O stretching (broad) vibration
900	914	P=O-H symmetric stretching
536	553	OH-P-OH bending
542	536	HO-P-OH bending vibration

#### 3.2. FTIR and FT-Ramanmolecular vibrational spectrum of PDPSC:

In order to analyzed the presence of molecular functional groups and qualitatively in the grown crystal. The FTIR spectrum has shown recorded 4000 to 400 cm<sup>-1</sup> using A IR

TRACER 100 Spectrometer by KBr pellet technique [21]. The observed resultant is shown in **Fig. 2**. The broad band at 3660cm<sup>-1</sup> in FT-IR and 3632<sup>-1</sup> cm in FT-Raman spectra are attributed is due to O-H free stretching vibrations. The asymmetric stretching vibration of P-O-OH group is assigned to the wavenumbers 2941cm<sup>-1</sup> in FT-IR and 2926<sup>-1</sup> cm in FT-Raman spectra. The asymmetric stretching mode O=P-OH group is identified to the wavenumbers 2436 cm<sup>-1</sup> in FT-IR and 2428 cm<sup>-1</sup> in FT-Raman spectrum respectively. The P=O stretching is found to appear at peaks 1300 cm<sup>-1</sup> and 1260 cm<sup>-1</sup> in IR and Raman spectra. The strongest peaks at 1097 cm<sup>-1</sup> and 1094 cm<sup>-1</sup> is attributed to P=O stretching (broad). The peaks at 900 cm<sup>-1</sup> and 914 cm<sup>-1</sup> are appears at P=O-H symmetric stretching. The peak at 536 cm<sup>-1</sup> and 553cm<sup>-1</sup> is attributed to HO-P-OH bending in FT-IR and FT-Raman counterpart[21].

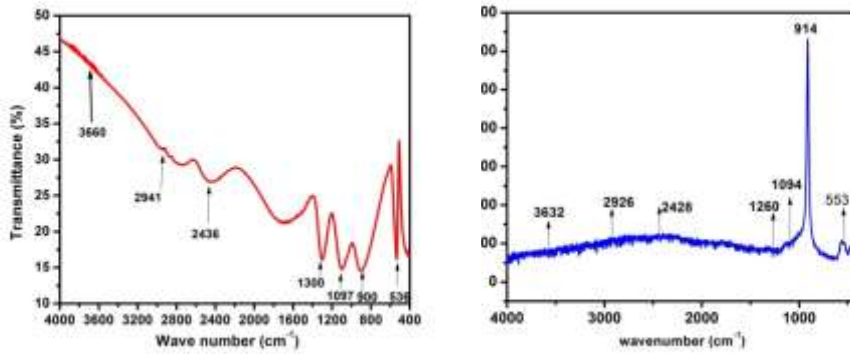


Fig. 2. (a) FTIR Spectrum of PDPSC (b) FT-Raman spectrum of PDPSC

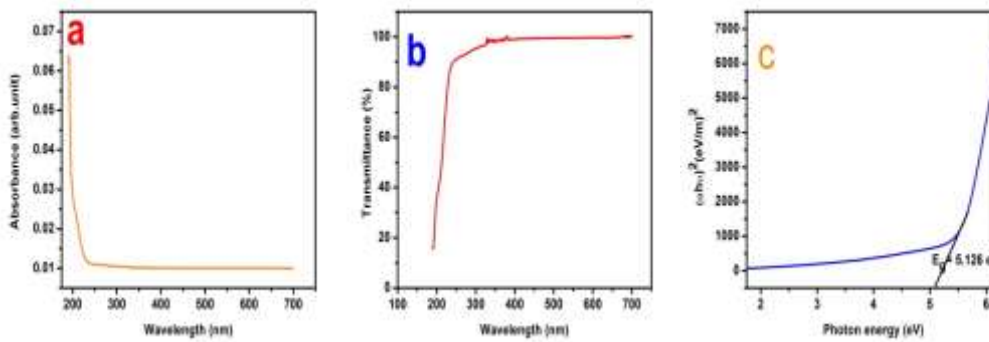


Fig. 3. (a) UV-Visible absorbance (b)Optical Transmittance spectrum(c) Tauc's plot of PDPSC

### 3. 3. UV-Vis optical studies

The optical properties of solids provide an important tool for studying energy bend structure, impurity levels, excites, localized defects, lattice vibrations and certain magnetic excitations. The optical absorption spectrum for the grown crystal value reports has been in the range 190-700 nm using variation Cary 5E (UV-Visible) NIR in spectrophotometer. The resulting spectrum is shown in **Fig. 3. (a)** Observed that there is low absorbance in the entire visible region and shows the extended transparency towards UV and IR regions. This is one of most desirable properties of NLO materials for device fabrications. The optical Transmittance spectrum of potassium dihydrogen phosphate doped sodium chloride crystal is shown in **Fig. 3. (b)**. This property is used to understand the electronic structure of the optical band gap of the synthesized crystal. From the transmittance spectrum, it is observed that the grown crystal totally transparent in the UV and visible spectral regions with the lower cut off wavelength around 240 nm there by confirming the advantages of the crystal. Complete transparency of the crystal between the region 190 nm to 700 nm. Advantages of the synthesized single crystal used for optoelectronics and nonlinear optical applications [22-25]. The lower cut off wavelength also observed at 240 nm suggest the suitability of this NLO material generating blue violet light using a diode laser. From the UV -Vis spectral study it can conclude that PDPSC as good transmission in UV and visible region, which is an added advantage for the crystal to be used in optoelectronic applications. The optical electronic band gap ( $E_g$ ) of the material is very closely related to the atomic and electronic band structures [26].

$$\alpha = \frac{2.3026 \log(1/T)}{t} \tag{A}$$

Where t is the thickness of the sample, T is the transmittance. The absorption coefficient ( $\alpha$ ) was evaluated using the above formula.

$$h\nu\alpha = A (h\nu - E_g)^{1/2} \tag{B}$$

In the above equality  $A$  is a constant,  $E_g$  is electronic band gap energy,  $h$  is the plank's constant,  $\nu$  is frequency of the incident photon. The electronic band gap energy of PDPOAD single crystal was evaluated from linear part of the  $\text{tauc}^2$ 's plot by plotting  $(h\nu\alpha^2) = 0$  gives the values of dielectric electronic band gap energy  $E_g = 5.126 \text{ eV}$  as shown in **Fig. 3. (c)**. Hence, this grown PDPOAD crystal processing such wide optical band gap can be an effectively used as a suitable candidate for UV tunable laser and NLO opto electronic applications.

### 3. 3. 1. Determination of optical constants

The refractive index ( $n_0$ ) is significant for frequency doubling experiments and the calculation of optical parameters when utilizing nonlinear optical (NLO) crystals. The other miscellaneous optical constants were calculated using the following theoretical formulae [26]. Extinction coefficient ( $K$ ) can be determined from the following relation:

$$K = \frac{\alpha\lambda}{4\pi} \quad (\text{C})$$

the reflectance ( $R$ ) in terms of optical absorption coefficient ( $\alpha$ ) and refractive index ( $n_0$ ) can be evaluated from the relation:

$$R = 1 \pm \frac{\sqrt{1 - \exp(-\alpha t) + \exp(\alpha t)}}{1 + \exp(-\alpha t)} \quad (\text{D})$$

$$n_0 = - \left\{ \frac{(R+1) \pm \sqrt{3R^2 - 10R - 3}}{2(R-1)} \right\} \quad (\text{E})$$

From **Fig. 4(d)**, it is clear that the reflectance ( $R$ ) and the extinction coefficient ( $K$ ) strongly depend on the high photon energy [26]. **Fig. 4(e)** represents the twain reflectance and extinction coefficient dependence on absorption coefficient. The internal energy of the device fully depends on this absorption coefficient ( $\alpha$ ). The refractive index ( $n_0$ ) determines how much light is bent, or refracted, when enters the material. Since the internal efficiency of the device depends on the incident photon energy ( $h\nu$ ), by carefully tailoring the  $\alpha$ -value and tuning the  $E_g$  of the material, where both happens together one can achieve the desired material meant to fabricate the optoelectronic devices. **Fig. 4(f)** exhibits the variation of refractive index ( $n_0$ ) with photon energy ( $h\nu$ ). From the figure it is clear that refractive index ( $n_0$ ) decreases with increase of photon energy ( $h\nu$ ). This lowering of refractive index emphasize that the PDPSC crystal exhibit the regular dispersion behavior. The calculated linear refractive index ( $n_0$ ) evaluated is 2.017 for the PDPSC crystal at  $\lambda_{\text{exc}} = 340 \text{ nm}$ . The high optical transparency and low refractive index of PDPSC in the UV-visible region makes it a prominent material for antireflection coating in solar thermal devices and NLO applications [26].

The photonic response of optical conductivity ( $\sigma_{op}$ ) of the material when irradiated with light is relevant to the refractive index ( $n_0$ ) and the speed of light ( $c$ ) as follows,

$$\sigma_{op} = \frac{n_0\alpha c}{4\pi} \quad (\text{F})$$

and also the electrical conductivity is correlated to the optical conductivity of the PDPSC crystal as follows,

$$\sigma_{ele} = \frac{2\lambda\sigma_{op}}{\alpha} \quad (\text{G})$$

**Fig. 4 (g)** illustrates that the optical conductivity ( $\sigma_{op}$ ) increases with photon energy ( $h\nu$ ), having high magnitude ( $10^8 \text{ } (\Omega \text{ m})^{-1}$ ) thus ratifying the presence of high photo response nature of the material [26]. From **Fig. 4(g)** and **Fig. 4(h)** it is suggested the low extinction value ( $10^{-5}$ ) and electrical conductivity ( $8 \times 10^{10} \text{ } (\Omega \text{ m})^{-1}$ ) highlight the semiconducting nature of the material. Hence this material is prominent for device applications in computing ultrafast optical data [26].

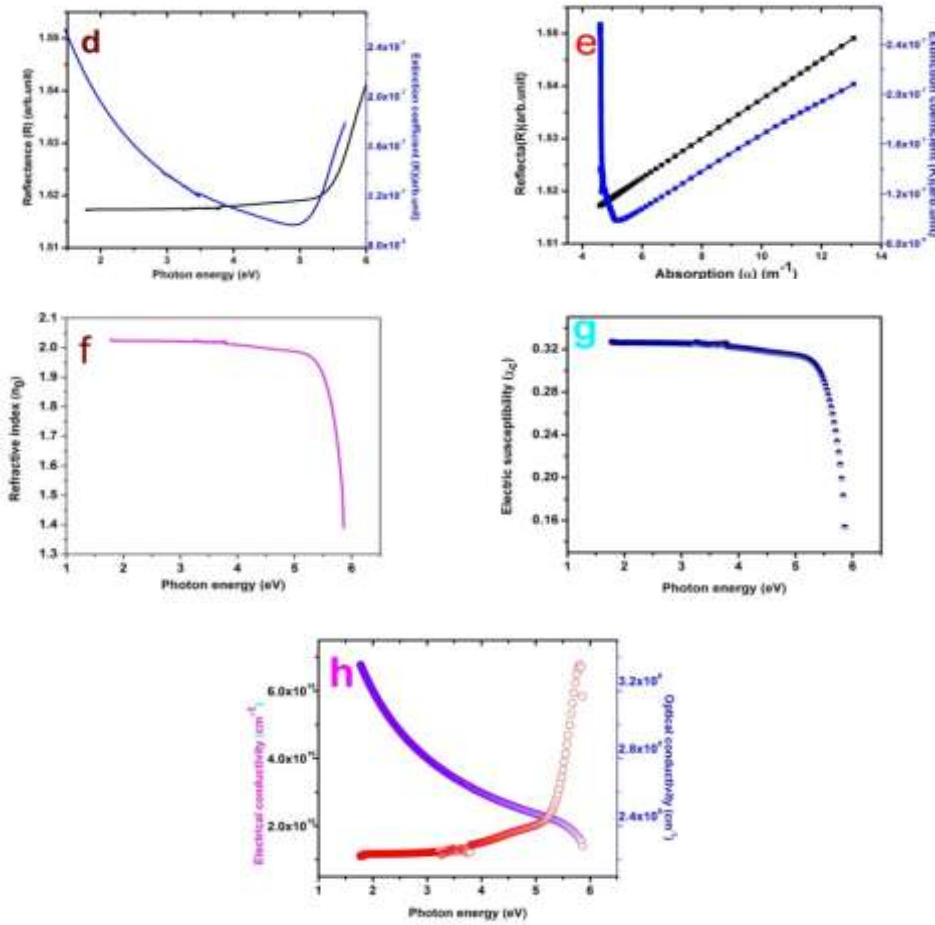


**Fig. 4.** (d) Plot of reflectance (R) and extinction coefficient (K) vs. photon energy (e) Variation of reflectance (R) and extinction coefficient (K) with absorption coefficient ( $\alpha$ ) (f) Plot of refractive index ( $n_0$ ) vs. photon energy (g) electric susceptibility ( $\chi_e$ ) vs. photon energy (f) Variation of electrical conductivity and optical conductivity vs. photon energy.

The electric susceptibility ( $\chi_e$ ) is closely related to optical constants given by [26],

$$\epsilon_r = \epsilon_0 + 4\pi\chi_e = n_0^2 - K^2 \quad (H)$$

$$\chi_e = \frac{n_0^2 - K^2 - \epsilon_0}{4\pi} \quad (I)$$

where  $\epsilon_0$  is the dielectric constant in the absence of any contribution from free carriers. The calculated value of electric susceptibility  $\chi_e$  is **0.3241** at  $\lambda= 340 \text{ nm}$  (Fig. 4(h)).

The real ( $\epsilon_r$ ) and imaginary part ( $\epsilon_i$ ) of the dielectric constants can be evaluated from the following relations:

$$\epsilon = (n_0 + iK)^2 (J)$$

$$\epsilon = n_0^2 - K^2 + 2in_0K = \epsilon_r + i\epsilon_i (K)$$

where

$$\epsilon_r = n_0^2 - K^2 \text{ and } \epsilon_i = 2n_0K \quad (L)$$

The value of real ( $\epsilon_r$ ) and imaginary part ( $\epsilon_i$ ) of the dielectric constants at  $\lambda= 340$  nm are 4.0715 and  $5.126 \times 10^{-7}$  respectively. Hence the optical constant of a material such as large value of electronic band gap, low value of extinction coefficient and refractive index are quite important to examine the material's potential in optoelectronic applications [26].

### 3. 3. 2. Urbach energy

In the exponential-edge region, the absorption coefficient below the fundamental absorption edge for the crystalline materials exhibit an exponential dependence on the photon energy ( $h\nu$ ) which is expressed by the so called Urbach relationship [26],

$$\alpha(h\nu) = \alpha_0 \exp\left(\frac{h\nu}{E_u}\right) \text{ (M)}$$

where  $\alpha_0$  is a constant and  $E_u$  the Urbach energy, which gives information about depth-of tail levels extending in to the forbidden electronic band gap below the absorption edge,  $h$  is a Planck's constant and  $\nu$  is the frequency of radiation. Whenever the degree of crystallinity increases, the slope of this region will increase. The observed slope **0.17972** of the linear portion of the plot was found from logarithm of the absorption coefficient ( $\ln(\alpha)$ ) with function of high photon energy ( $h\nu$ ) which interprets that the crystal is highly crystalline in nature. Urbach energy  $E_u$  was calculated by taking the reciprocal of the slope of linear portion of the plot drawn between  $\ln(\alpha)$  and  $h\nu$  depicted in **Fig. 5**. The calculated Urbach energy value is **5.5642eV** for PDPSC crystal. The low value of Urbach energy (**5.5642eV**) is an indicative of decrease in structural defect in as-grown PDPSC crystal, supports its good NLO performance.

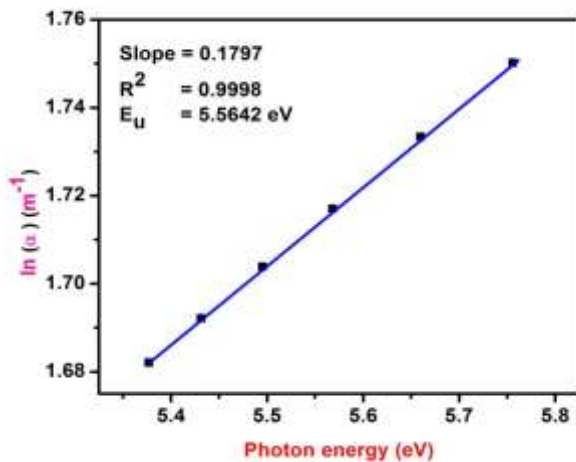


**Fig. 5.** Plot  $\ln(\alpha)$  vs.  $h\nu$  for the PDPSC.

### 3. 4. Surface morphology investigated by SEM

The surface morphology nature of the grown crystal analysis had been studied by scanning electron microscope. Carbon coating has applied for the sample before subjecting the crystal surface to electron beam to make a non-conductive specimen. During recording the image through SEM the appropriate coating is necessary to provide good conductivity and for the good field emission of secondary electrons. It can be observed that the grown crystal has cracks and few inclusions which may be due to the impact of growth conditions. The SEM images in figure shows Nano bricks like morphology. The different morphology expose subjected in a  $\mu\text{m}$  of the composite Nano bricks morphology of the as-synthesized sample. It is homogenous in nature with good clarity as shown in **Fig. 6**.

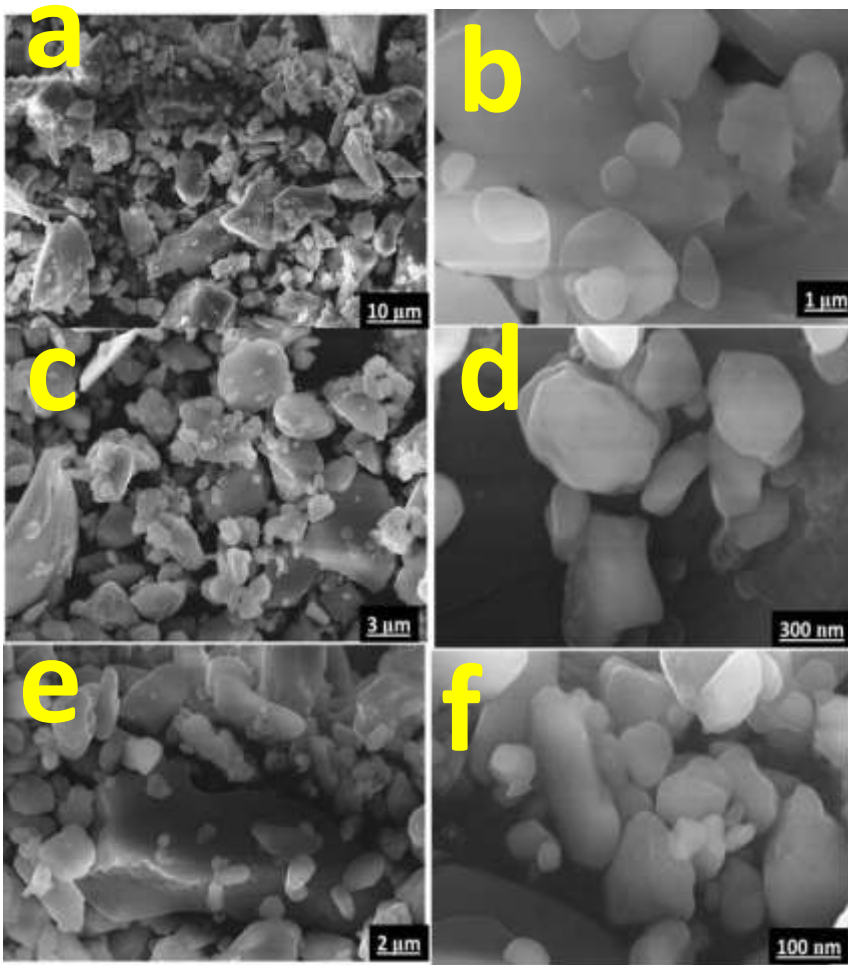


Fig. 6. Typical view of SEM images of PDPSC single crystal.

### 3. 5. EDAX:

The crystalline or elemental chemical composition of the grown crystal was examined by Energy Dispersive X-ray (EDAX) Analysis spectrometer. The EDAX spectrum is resulting from the electron back scattering. Further the obtained spectrum of energy versus relative counts of the X-rays gives the quantitative information about the elements presents present in the testing sample. It reveals the presence of O, Na, P and K (oxygen, sodium, phosphorus and potassium) with the weight percentage of 55.44%, 1.12%, 7.62%, 23.48 % and 23.05% as shown in **Fig. 7**.



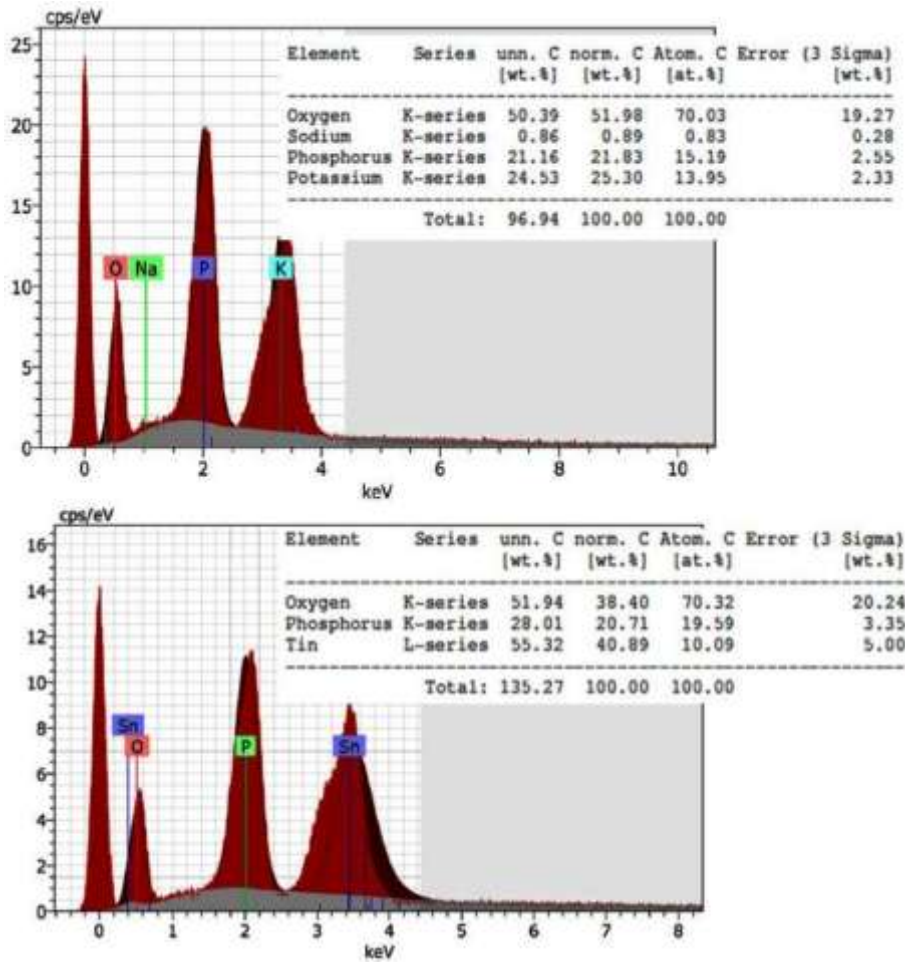


Fig. 7. EDAX Compositional spectrum of PDPSC

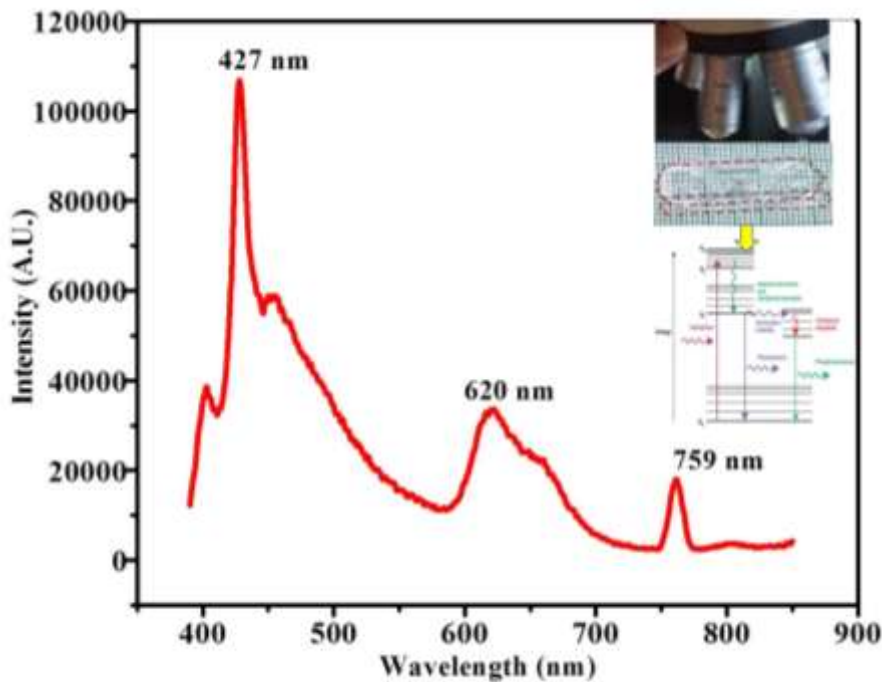


Fig. 8. Fluorescence lifetime spectrum of PDPSC

### 3. 6. Photoluminescence study

Photoluminescence (PL) Spectrograph is one of the Non-destructive tools to understand the electronic energy band structure of material [27]. Basically, the luminescence phenomenon indicates the presence of intrinsic behavior in the forbidden band of PDPSC crystal. PL is carried out by PERKINELMER LS 45 Spectrofluorophotometer and excitation source used was xenon arc lamp (150w). A broad PL Spectrum have been obtained from PDPSC in the wavelength range of emission spectrum 350nm to 900 nm (3.54-1.37eV) is shown in Fig. 8. The excitation wavelength 240nm chosen from UV-Visible study is identified from the value of optical band gap. The result shows that PDPSC crystal has one peak of violet emission at 427nm (2.90eV). The obtained two peaks corresponding to appeared Green emission one with high PL intensity at 620 nm (2.00eV) and other with weak shoulder corresponding to the decreased PL intensity at 759nm (1.63eV). The material with photoluminescence of violet and green emissions are found to be more useful for OLED (An organic light-emitting diode) application [28].

### 3. 7. Thermal analysis (TG/DSC):

The thermal behavior of PDPSC need to add examined by thermo gram metric analysis (TG) and differential scanning calorimetric (DSC) by taking sample of 5.419mg at the beginning. The NETZS CH STA 449F3 thermal analyzer played to vital role was employed at a heating rate 20°C/min in the Nitrogen atmosphere[29]. The thermo gram obtained from TG/DSC analyses recorded at 20-1200°C is shown in Fig. 9. From the TGA profile we observe that there is no weight loss up to 220°C in the grown crystals. There after weight loss occurs in a single step between inflection 268.4°C to 781.6°C which gradually decreases to Residual mass 1399.2°C (77.82%) .The differential Scanning Calorimetric (DSC) curve shows sharp endothermic peaks at 250°C(PDPSC) reveals the melting point respectively ensures maximum , temperature for NLO application for this crystal is limited to 220°C.

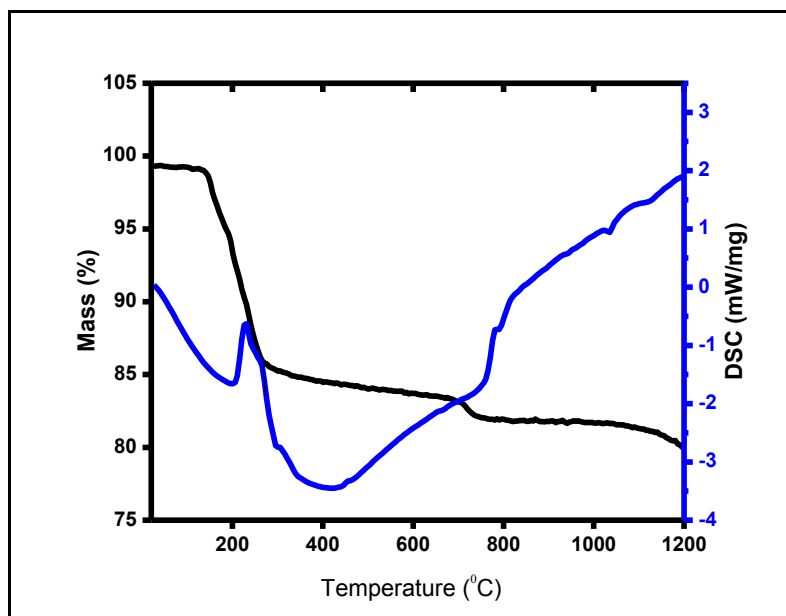


Fig. 9. TG and DSC curves of PDPSC

### 3. 8. Non-Linear Optical (NLO) Test

Second harmonic generation (SHG) efficiency is one of the second order nonlinear optical property and its value was found for the powder sample of PDPSC Using Kurtz and Perry powder technique [30], and the efficiency of PDPSC sample was compared with the microcrystalline powder of KDP. Kurtz and Perry by passing the output of angle tuned and temperature stabilized Second harmonic and Third harmonic Generation laser beam of wavelength 1064nm. A Q switched High Energy Nd :YAG Laser (QUANTA RAY Model LAB – 170 -10) Model HG-4B- High efficiency, beam of wavelength was used with pulse width of 8ns and the repetition rate being 10 Hz. Photodiode and oscilloscope assembly examined the output light from the sample.

The SHG output is (532 nm) is finally detected by a photomultiplier tube and displayed on the oscilloscope. The SHG efficiency was found to be 1.22 times of KDP.

#### 4. Conclusion

Optically good quality crystals of PDPSC crystals have been grown by slow evaporation method. UV-Vis spectra showed that grown crystal has been optically transparent through 190-700 nm and hence suggests the suitability of this material for optical devices. Single X-ray diffraction analysis confirms the crystalline lattice parameters of the grown crystal. The FTIR spectral analysis confirm by identification of the functional group presence in the crystal. Non Linear Optical evaluation is 1.61 (milli joule) less than that of KDP. The TG/DSC analyses confirmed that the material is stable up to 1300. Photoluminescence spectral study revealed the electron excitation in the grown PDPSC.

#### Acknowledgements

The authors **G.M & S. J** expresses her sincere thanks for the scientific supports extended by sophisticated analytical instruments facility SAIF, Indian Institute of Technology IIT-Madras, Chennai for support in single XRD, TG/DSC, PL, measurement and the facilities rendered by Department of Polymer and Nano science of B.S. Abdur Rahman university (BSAU), Chennai for providing SHG measurement. Also Thanks to Kalasalingam University for support in FTIR, SEM &EDAX measurements.

#### References

1. Ramasamy. P, SanthanaRaghavan, Crystal growth processes and methods, KRU Publications, Kumbakonam (1999)
2. Dmitriev. V.G, Gurzadyan.G.G, Nicogosyan.D.N, Hand Book of nonlinear optical Crystals, New York: Springer Verlag: 1999.
3. Wong.M.S, Bosshard Pan.F C, Gunter.P,Adv Mater 8 (1996) 677.
4. Warren.L.F, Electronic materials our future, in: Allred.R.J. , Martinez.K.B, Wischmann (Eds), Proceedings of the Fourth International Sample Electronics Society for the Advancement of Materials and Process Engineering, vol. 4, Covina, CA, 388 (1990).
5. Zyss.J, Nicoud.J. F, Coquilly.M.J, Chem. Phys. 81 (1948) 4160.
6. Ledoux.I, Badan.J, Zyss.J, Migus.A, Hulin.D, Etchepare.J, Grillon.G, Antoinette.J, Opt Soc AM: B. 4 (1987) 987.
7. Shirsat.M.D, Hussaini.S.S, Dhumane.N.R, Dongre. V.G, Cryst. Res. Technol. 43 (2008) 756-761.
8. Kannan.V, Bairava Ganesh.R, Sathyalakshmi. R, Rajesh.N.P, Ramasamy.P, Mater. Lett, 56 (2002) 578.
9. Zaitseva.N. P, Rashkovichand.L.N, Bogatyreva.S.V, J. Cryst.Growth. 48 (1995) 276-282.
10. Mark.A, Rhodes, Woods.B, De Yoreo.J. J, Roberts.D, Atherton.L. J, J. Appl. Opt. 134 (1995) 5312-5325.
11. Balamurugan.S, Ramasamy. P, Inkong. Y. P, Manyum. P, Mater. Chem. Phys. 113 (2009) 622-625.
12. Dixit.V. K, Rodrigues.B.V, Bhat.H. L, Bull, Mater.Sci. 24 (2001) 455-59.
13. AnandaKumari.R, Chandramani.R, Bull. Mater. Sci. 26 (2003) 255-259.
14. Priya. M, Padma.C.M, Freeda.T.H, Mahadevan.C.K and Balasingh.C, Bull.Mater.Sci, Vol 24 (2001) 511-514.
15. Parikh.K.D, Dave.D.J, Parekh.B.B, Joshi.M.J, Bull.Mater.Sci, 30 (2007) 105-112.
16. Dhanaraj.P.V, Mahadevan.C.K, Bhagavannarayanan.G, Ramasamy.P, Rajesh.N.P, J. Cryst.Growth, 310 (2008) 5341-5346.
17. Kumeresan.P, MoorthyBabu.S, Anbarasan.P.M, J.Cryst. Growth, 310 (2008) 1999 - 2004.
18. Dhanaraj.P.V, Rajesh.N.P, Mahadevan.C.K and Bhagavannarayana.G, Physica B, 404, (2009) 2503-2508.
19. Parikh.K.D, Dave.D.J, Parekh.B.B , Joshi.M.J, Cryst. Res. Technol, 45 (2010) 603-610.
20. Ambhore.P. S, Gambhire.A.B, Devade.S.K, Muley.G.G, crystal structural and SHG efficiency study on Nacl doped KDP crystals, Int. J Basic & Appl. Res. 230-233 (2012).
21. Alosious Gonsago.C, Helen Merina Albert, Janarthanan.S, Joseph ArulPragasam. A, Int. J. App. PhyMaths, 2, 422-425.

22. Loretta.F, Josephine Rani.T, Selvarajan.P, Perumal. S, and Ramalingam. S, World J. Sci.Technol 3 (2009) 1.
23. Rahman. A, and Podder. J, Int. J. Optics, 86 (2010) 15.
24. Krishna Kumar. V, and Nagalakshmi.R, Spectrochim. Acta, Part A, 61 (2005) 499.
25. Venkataramanan.V, Maheswaran.S, Sherwood.J. N, and Bhat.H. L, J. Cryst. Growth, 179 (1997) 605
26. Krishna Kumar. V, Guru Prasad.L, Nagalakshmi. R, Eur. Phys. J. Appl. Phys. 48 (2009) 20403 – 20409.
27. Kalaivani.D, Vijayalakshmi. S, Elberin Mary Theras. J, Jayaraman. D, Joseph. V, Growth of L-Valinium Aluminum Chloride Single Crystal for OLED and super capacitor applications, Opt. Mater.50 (2015) 87-91
28. Mahakhode. J.G,Bahirwar. B. M, Dhoble. S. J, Moharil. S.V, in: Proceedings of the ASID, New Delhi, and October 8-12, 2006.
29. Kurtz. S.K, Perry. T.T, Powder technique for the evaluation of nonlinear optical Materials, J. Appl. Phys. 39 (1968) 3798-3813.

\*\*\*\*\*